Proceedings World Geothermal Congress 2020+1
Reykjavik, Iceland, April - October 2021

# Solute Geothermometry Applied to Low-Medium Enthalpy Geothermal Systems

María Olguín[1*], Loic Peiffer[1], Claudio Inguaggiato[1], Christoph Wanner[2], Patrick Dobson[3], Nicolas Spycher[3] and Thomas Kretzshmar[1]

[1]Departamento de Geología, CICESE, Ensenada, B.C., México

[2]Institute of Geological Sciences, University of Bern, Bern, Switzerland

[3]Energy Geosciences Division, Lawrence Berkeley National Laboratory, Berkeley, CA, USA

[*]olguinm@cicese.edu.mx

**Keywords:** Geothermometers, temperature, geothermal fluids

**ABSTRACT**

One of the most useful tools to estimate the temperature of deep geothermal reservoirs and reduce the costs of exploratory drilling is solute geothermometry, which is based on the chemical analysis of a fluid sampled from a thermal spring or well. The basic assumption of solute geothermometry is that the geothermal fluid reaches chemical equilibrium with certain minerals within the reservoir, and subsequently flows toward the surface without substantially changing its chemical composition. Accordingly, the concentrations in dissolved elements reflect the thermal conditions at depth. The most commonly applied geothermometers (called "classical") are based on the absolute concentration of one dissolved species, like silica ($SiO_2$), or on the concentration ratio of several dissolved elements such as the sodium-potassium (Na-K), sodium-potassium-calcium (Na-K-Ca) or potassium-magnesium (K-Mg) ratio. In contrast to classical geothermometers, multicomponent geothermometry computes the saturation indices of selected minerals expected in the geothermal reservoir over a wide range of temperatures based on full water analyses. The reservoir temperature is then estimated by the clustering of these saturation indices around zero.

For this contribution, we first perform reactive transport simulations to create a wide range of synthetic conditions and further test the response of solute geothermometers. Second, we evaluate the response of classical geothermometers and multicomponent geothermometry when applied to low–medium enthalpy geothermal systems (with reservoir temperatures below 180°C). Under such thermal conditions, the kinetics of dissolution/precipitation reactions are slower than at higher temperatures, and hence, the condition of equilibrium may not be achieved. Our evaluation of solute geothermometry was conducted using a database including water chemical compositions (182 analyses) and measured reservoir temperatures. Our results indicate that Na-K based geothermometers provide acceptable temperature estimates ($T_{estimated} - T_{measured} = \pm 20$°C) for only ~ 4% of the fluid compositions. Higher rates of acceptable estimates (up to 60%) are obtained with the multicomponent method when using fixed selected mineral lists for computing the saturation indices. We consider this result as promising considering that we did not perform a case-by-case analysis of each geothermal system contained within the database.

## 1. INTRODUCTION

Solute geothermometers have been used for many years to estimate geothermal reservoir temperatures as a low-cost alternative to exploratory drilling. The most common applied solute geothermometers (called "classical") are based on the solute concentration of dissolved species, like silica ($SiO_2$) (Fournier, 1977; Fournier and Potter, 1982) or the concentration ratio of several dissolved elements, such as the sodium-potassium (Na-K), sodium-potassium-calcium (Na-K-Ca), or potassium-magnesium (K-Mg) ratio (Fournier and Truesdell, 1973; Giggenbach, 1988), as it is shown in Table 1. In contrast to classical geothermometers, the multicomponent geothermometry method, developed by Reed and Spycher (1984), computes the saturation indices (SI) of selected minerals expected in the geothermal reservoir over a wide range of temperatures based on full water analyses. In particular, the SI of a specific mineral is given as:

$$SI = \log\left(\frac{Q}{K}\right) \tag{1}$$

where $Q$ is the ion activity product and $K$ the mineral solubility constant. The SI are graphed as a function of temperature, and the reservoir temperature is then estimated by the clustering of these saturation indices around zero (the chemical equilibrium point).

Classical geothermometers have proved to be reliable tools to infer the temperature of high-enthalpy geothermal reservoirs, in which the geothermal waters reach chemical equilibrium with various aluminosilicates, such as K-feldspar or albite (Fournier, 1977, 1981; Giggenbach, 1983, 1988, among many others). The two main assumptions for a successful application of these geothermometers are: (1) the reservoir fluid reaches equilibrium with the minerals involved in the geothermometer formulation, (2) the fluid does not re-equilibrate during its upflow to the surface, due to mineral dissolution-precipitation. However, in low to

medium enthalpy geothermal reservoirs, the kinetics of water-rock reactions are slower, which make full equilibrium between fluids and the reservoir minerals less common (White, 1970; Fournier et al., 1974; Truesdell, 1976; Fournier, 1977; 1989; Ellis, 1979). Hence, classical geothermometers usually fail in estimating temperature of low to medium enthalpy geothermal reservoirs. In this matter, multicomponent geothermometry is more flexible because the user can choose the mineral assemblage to consider in temperature computations (e.g., Palmer et al., 2014).

The main goal of this study is to evaluate the response of classical and multicomponent geothermometry when applied to low-medium enthalpy geothermal systems. We first investigate theoretically the reach of each type of geothermometer through a reactive transport model simulating advanced argillic alteration, occurring within a medium-enthalpy reservoir. In this model, fluid compositions with different chemical equilibrium states are generated and used to compute both classical and multicomponent geothermometry. We only simulate chemical reactions within the reservoir, and do not consider secondary processes associated with fluid upflow towards the surface (assumption 2 described previously). The multicomponent analysis is performed using the GeoT software (Spycher et al., 2014), the results of which are described in Section 3. We them use a database with more than 180 water compositions from low to mid-enthalpy geothermal systems, including measured bottom-hole temperature, to test the sensitivity of the multicomponent approach to different mineral groups. Because the database lacks Al concentrations for these fluids, we use an updated version of GeoT named iGeoT (see Section 3) to estimate this parameter through numerical optimization.

**Table 1: Classical geothermometers used in this research**

| Geothermometer | Equation | Temperature range of applicability | Reference |
|---|---|---|---|
| $SiO_2$ (quartz) | $T^a = -42.198\ (\pm1.345)+0.28831(\pm0.01337)S - 3.6686\times10^{-4}\ (\pm3.152\times10^{-5})S^2 + 3.1665\times10^{-7}\ (\pm2.421\times10^{-7})S^3 + 77.034(\pm1.216)\log S$ | 150 - 330°C | Fournier and Potter (1982) |
| $SiO_2$ (amorphous silica) | $T^a = [731 / (4.52 - \log S)] - 273.15$ | 20 - 250°C | Fournier (1977) |
| $SiO_2$ (chalcedony) | $T^a = [1032\ (4.69 - \log S)] - 273.15$ | 20 - 250°C | Fournier (1977) |
| Na-K-Ca | $T^a = [1647 / (\log10(Na / K) + \beta[\log10((Ca / Na)1/2) + 2.06] +2.47)] - 273.15$ | 4 - 340°C | Fournier and Truesdell (1973) |
| Na-K | $T^a = [1390 / (\log10(Na / K) + 1.75)] - 273.15$ | >180°C | Giggenbach (1988) |
| K-Mg | $T^a = [4410 / (14.0 - \log (K^2 / Mg))] - 273.15$ | >180°C | Giggenbach (1988) |

[a] Temperature (T) in °C.

$\beta = 4/3$ for $T < 100$°C; $\beta = 1/3$ for $T > 100$°C

$S$ is the concentration of $SiO_2$ in mg/kg

## 2. REACTIVE TRANSPORT SIMULATIONS

Reactive transport simulations were performed to create a synthetic hydrothermal system testbed to evaluate the response of both classical and multicomponent geothermometers. We opted to simulate a case of advanced argillic alteration for the following reasons. This relatively common alteration type is associated with steam-heated acid-sulfate waters and can occur under low-to-medium temperature conditions (Reed, 1997). Furthermore, the mineral assemblage considered in the classical Na-K geothermometer formulation (Na and K-feldspars) are usually fully altered when this type of alteration occurs. It is hence a worst-case scenario for applying Na-K geothermometers, and an ideal one for testing the potential of the multicomponent method. In particular, we simulated the alteration of muscovite and paragonite into kaolinite (Kuhn et al., 2004):

$$2NaAl_3Si_3O_{10}(OH)_2 + 2H^+ + 3H_2O \rightarrow 3Al_2Si_2O_5(OH)_4 + 2Na^+ \quad (2)$$

paragonite kaolinite

$$2KAl_3Si_3O_{10}(OH)_2 + 2H^+ + 3H_2O \rightarrow 3Al_2Si_2O_5(OH)_4 + 2K^+ \quad (3)$$

muscovite kaolinite

A description of the simulator, model geometry, fluid flow and mineralogical conditions are presented in the following sections.

### 2.1 Numerical simulator

Water-rock reaction simulations were performed with TOUGHREACT V3 (Xu et al., 2014), a numerical simulation program for reactive chemical transport under kinetic or equilibrium conditions. It is based on the non-isothermal multi-phase and heat flow simulator TOUGH2 (Pruess, 1991). We used the equation of state module EOS1 to simulate fully saturated, isothermal water flow occurring as a single phase only.

### 2.2 Modeling approach

We simulate reactive transport along a 200 m long 1D horizontal mesh, discretized into 200 grid blocks of 1 $m^3$ volume (Figure 1). The model domain aims in representing an aquifer with a constant initial lithology, through which an acid-sulfate water progressively transforms a paragonite and muscovite-bearing mineral assemblage into kaolinite (reactions 2 and 3). In this simplified model, we consider isothermal conditions (150°C along the model) and a pressure of 10 bars in the first grid block. These T-P values allows to simulate single phase fluid (no boiling) conditions. A high permeability of $10^{-12}$ $m^2$ and a porosity of 0.1 was assigned to the entire synthetic aquifer. A boundary element with very large volume (>$10^{50}$ $m^3$) was assigned to the end of the column in order to fix pressure and temperature boundary (at 10 bars, and 150°C, respectively).

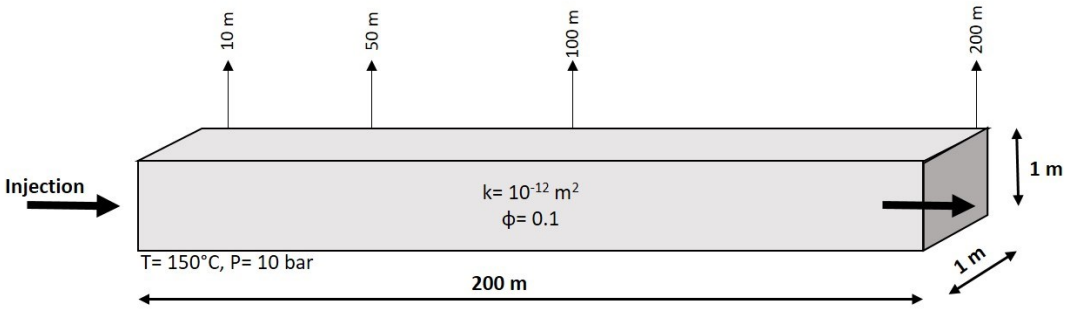


**Figure 1: Conceptual aquifer used to simulate reactive transport. 10 m, 50 m, 100 m and 200 m arrows indicate synthetic fluid sampling points.**

A source term is assigned to the left-hand boundary block to induce fluid flow within the domain, at a low velocity (~$1.25\times10^{-6}$ m/s). The injected water of acid-sulfate composition corresponds to a geothermal steam-heated water from the Krýsuvik geothermal area in Iceland (Table 2, Kaasalainen and Stefánsson, 2012). The initial water filling the aquifer has a composition corresponding to surface water from Thjórsá river, Iceland (Table B-1, Kaasalainen and Stefánsson, 2012).

**Table 2: Chemical composition of initial (1) and injected (2) waters (from Kaasalainen and Stefánsson, 2012). Concentrations in mg/l.**

| # | T (°C) | pH | $SiO_2$ | Na | K | Mg | Ca | Cl | $SO_4$ | Al |
|---|---|---|---|---|---|---|---|---|---|---|
| 1 | 150 | 7.45 | 11.5 | 7.79 | 0.47 | 1.41 | 3.89 | 3.37 | 4.8 | 0.01 |
| 2 | 150 | 2.02 | 384 | 150 | 2.48 | 31.2 | 31.2 | 5.2 | 3407 | 258.9 |

In order to simulate reactions (2) and (3), we assign an arbitrary abundance of paragonite and muscovite to the entire model domain (Table 3). Kaolinite is initially absent and progressively forms over the simulation period when the two original minerals interact with the injected acid fluid. Silica is assumed to be present initially as chalcedony. As carbonates and sulfates are common minerals in geothermal systems (Wanner et al., 2017), initial abundances of calcite and gypsum are also included in the model (Table 3).

**Table 3: Initial mineralogical composition used in simulations**

| **Mineral** | Paragonite | Muscovite | Kaolinite | Chalcedony | Calcite | Gypsum |
|---|---|---|---|---|---|---|
| **Abundance (vol. %)** | 20 | 20 | 0 | 40 | 10 | 10 |

Mineral dissolution and precipitation are simulated under kinetic conditions, following Lasaga et al. (1994) and Steefel and Lasaga (1994) general expression:

$$r = A \cdot k_{25}\left[\frac{E_a}{R}\left(\frac{1}{T}-\frac{1}{298.15}\right)\right]\cdot\left(1-\frac{Q}{K}\right) \quad (4)$$

where $r$ refers to the reaction rate (mol $kg_{H2O}^{-1}$ $s^{-1}$), $A$ is the specific reactive surface area per $kg_{H2O}$, $k_{25}$ is the reaction rate constant at 25°C (mol $m^{-2}$ $s^{-1}$), $Ea$ is the activation energy (kJ/mol), $Q$ is the ion activity product and $K$ is the equilibrium constant of the reaction (Table 4). A specific reactive surface area of 394 $cm^2/g$ was used for chalcedony, calcite and gypsum, while higher surface area of 6824 $cm^2/g$ was assigned to paragonite, muscovite, and kaolinite. These values were taken from Dobson et al. (2003). Reaction rate constants and activation energies were selected according to Palandri and Kharaka (2004). Finally, TOUGHREACT was run with the 'soltherm.H06' thermodynamic data by Reed and Palandri (2006). The simulation was run for a period of 1000 years, which was enough to reach steady-state conditions (Figure 2).

**Table 4: Equilibrium constants, reaction rate constants, activation energies and reactive surface areas of considered minerals dissolution/precipitation reactions.**

| Mineral | Log(K)[a] | $k_{25}$(moles $m^{-2}$ $s^{-1}$)[b] | Ea (kJ/mol)[b] | Surface area ($cm^2/g$)[c] |
|---|---|---|---|---|
| Paragonite | 12.415 | 1.00E-13 | 22 | 6824 |
| Muscovite | 8.708 | 2.81E-14 | 22 | 6824 |
| Kaolinite | 3.18 | 6.60E-14 | 22.2 | 6824 |
| Chalcedony | -3.728 | 3.92E-12 | 74.5 | 394 |
| Calcite | 1.816 | 1.54E-06 | 23.5 | 394 |
| Gypsum | -4.443 | 1.62E-03 | 0.0 | 394 |

[a] At 25°C, according to Soltherm.H06 database (Reed and Palandri, 2006).

[b] At 25°C, according to Palandri and Kharaka (2004).

[c] Taken from Dobson et al. (2003).

## 3. GEOT-IGEOT AND DATABASE ANALYSIS

Spycher et al. (2014) developed the GeoT software to automate the multicomponent approach. GeoT performs some statistical analysis of the SI curves to estimate the equilibrium temperature. In particular, it computes the median (RMED), mean (MEAN), standard deviation (SDEV) and root mean-square error (RMSE) of saturation indices as a function of temperature (Figure 3). Also, it computes the temperature spread (Tspread), which is the temperature interval defined by the saturation indices (at SI = 0) of the considered minerals. The estimated equilibrium temperature is given by the minimum median of absolute SI values. The user is allowed to specify a given number of "best-clustering" minerals to be considered in the temperature estimation. To select these minerals, GeoT eliminates all those minerals with SI above a value of 0.05 over the entire temperature range considered, and then, evaluates the median (RMED) of the remaining mineral SI at all temperatures. Finally, the program selects the of "best-clustering" minerals as the minerals showing the lowest RMED values over the entire temperature range. More recently, GeoT was coupled with iTOUGH2 (Finsterle and Zhang, 2011) to become iGeoT (Spycher and Finsterle, 2016). This updated version allows reconstruction of deep geothermal fluid compositions by numerical optimization of input parameters (e.g. aqueous and gas species concentrations, dilution fractions, and steam weight fractions).

We first process the composition of the synthetic water samples generated with TOUGHREACT using the most recent GeoT version 2.1. We assume that we do not have any knowledge on the mineral assemblage constituting the modeled aquifer nor on the thermal regime. Therefore, GeoT is run with a large list of minerals commonly found in low and high geothermal systems, such as zeolites, clays, micas, carbonates, feldspars, sulphates and $SiO_2$ polymorphs. This list is further referred as Group 6 (Table 4). As a natural geothermal fluid is not expected to equilibrate with a large amount of minerals (according to Gibb's Phase Rule), we ask GeoT to compute equilibrium temperature with only 6, "best-clustering", minerals. We expect that GeoT selects the same minerals that are specified in the reactive transport simulation (i.e. paragonite, muscovite, kaolinite, chalcedony, calcite and gypsum) to calculate reservoir temperature. Results from the simulation and GeoT analysis are discussed in Sections 4.1 and 4.2.

The second part of this study consists in testing the sensitivity of the multicomponent approach to using different mineral groups for calculating fluid-mineral equilibria. For this purpose, we analyzed a database with more than 180 water chemical compositions from geothermal wells sampled around the world, using only samples derived from wells with bottom-hole temperatures below 180°C. This database comes from a larger compilation by Kuhn et al. (2004). We ensured that each water analysis had a charge balance error within ±10%, a measured pH and reported concentrations in $Na^+$, $K^+$, $Mg^{2+}$, $Ca^{2+}$, $Cl^-$, $HCO_3^-$, $SO_4^{2-}$ and $SiO_2$. However, Al concentrations are mostly missing from the database. Because Al concentration is required for computing SI of aluminosilicates, we used iGeoT (v1.0) to estimate the Al concentration. This program performs parameter optimization through

the analysis of an objective function. This function is obtained from the difference between the model calculation and the observed data. Several minimization algorithms, implemented in iGeoT, allow to look for the minimum value of the objective function by iteratively updating the model parameters and determining the response of the model to variations of any input parameters. In this study, we used the grid search algorithm that provides a systematic evaluation of the objective function in a parameter space. In particular, we considered an objective function that takes into account the median (RMED) of saturation indices, as well as the spread of temperatures (Tspread). iGeoT therefore automatically looks for Al concentrations that minimize these two parameters. iGeoT is asked to search for an Al concentration within a range between 1 x $10^{-6}$ to 1 x $10^{-10}$ mol/L. This range, taken from Peiffer et al. (2014), was estimated by optimizing Al concentrations for a real geothermal field site (Dixie Valley, Nevada). Additionally, another methodology for constraining Al concentration was implemented. It is based on the approach presented by Pang and Reed (1998) named "Fix-Al" method, and consists of assuming that the concentration of Al is constrained by thermodynamic equilibrium with a selected Al-bearing solid phase over the entire considered temperature range. In this study, Al concentration was assumed to be controlled by equilibrating the fluid with microcline. The "Fix-Al" method was applied to the database considering the mineral group 6.

For analysis of the water samples from the geothermal database, we developed a code in Python language. This code modifies iGeoT input files to incorporate all the water compositions included in the database with the purpose of automating the program execution. Also, the code incorporates mineral lists defined by the user to the iGeoT input files. Finally, the code evaluates iGeoT results and determines if the geothermometers provide acceptable temperature estimates ($T_{estimated} - T_{measured} = \pm 20°C$). Similar to the reactive transport study, we assume that we do not have any knowledge of the thermal regime at depth and the type of reservoir minerals present. Therefore, iGeoT was run with different mineral groups commonly found in low and high temperature geothermal systems, such as zeolites, clays, micas, carbonates, feldspars, sulphates and $SiO_2$ polymorphs (Table 4). The first five groups contain 6 minerals, while, the last one (group 6) includes all the minerals from the other groups. This last group was previously used for the reactive transport modeling study. When iGeoT is run with the first 5 groups, it estimates the temperature considering all 6 minerals in these groups. When Group 6 is used, only the 6 "best-clustering" minerals are considered for temperature computation (automatic selection), with the condition that only one of the three $SiO_2$ phases (quartz, chalcedony and amorphous silica) is retained.

One relevant point is that we can only select minerals for which dissolved concentrations of their components are known (or can be estimated). That is, we can only use minerals whose compositions can be expressed by aqueous species considered in the simulations, namely $0Na^+$, $K^+$, $Mg^{2+}$, $Ca^{2+}$, $Cl^-$, $HCO_3^-$, $SO_4^{2-}$, $SiO_2$ and Al. Results from the database analysis by iGeoT are discussed in Section 4.3.

**Table 4: Mineral assemblages used in iGeoT**

| Group | Minerals |
|---|---|
| 1 | Quartz, microcline, albite, phlogopite, laumontite and anhydrite |
| 2 | Chalcedony, microcline, calcite, clinochlore, Na-clinoptinolite and kaolinite |
| 3 | Quartz, K-clinoptinolite, paragonite, Mg-beidellite, heulandite and dolomite |
| 4 | Chalcedony, albite, muscovite, stilbite, Mg-montmorillonite and gypsum |
| 5 | Amorphous silica, Na-montmorillonite, prehnite, K-beidellite, magnesite and albite |
| 6 | All the previous minerals |

For this analysis, the thermodynamic database SOLTHERM.H06 (Reed and Palandri, 2006) was employed.

## 4. RESULTS AND DISCUSSION

### 4.1 Reactive transport simulation

Saturation indices values were calculated for different water compositions sampled along the length of the simulated aquifer, at a time of 1000 years (end of simulation). Figure 2A shows the SI of the 6 minerals considered in the simulation. Within the first 10 meters of the modeled domain, the fluid is predicted to be undersaturated with respect to gypsum, calcite, muscovite, and paragonite, which means that these minerals dissolve. The injected acid-sulfate fluid is slightly supersaturated with respect to kaolinite, which precipitates. Muscovite and paragonite dissolution releases K, Na, Al and $SiO_2$ into solution. Kaolinite precipitation consumes Al and $SiO_2$. The coupled dissolution of paragonite and muscovite and precipitation of kaolinite consumes $H^+$. The $H^+$ consumption induces a progressive neutralization of the injected acidic fluid. The pH evolution along the mesh (Figure 2B) becomes stable (near pH 6.5) at 100 m, where the fluid reaches close-to equilibrium conditions with most minerals (Figure 2A). At this distance, the fluid is still slightly supersaturated with respect to kaolinite (SI= 0.097), and tends to reach full equilibrium with this mineral towards 200m. As chalcedony solubility does not depend on pH (at least below pH of 8, Rimstidt and Barnes, 1980; Rimstidt, 1997), the evolved fluid composition at 1000 years is at equilibrium with this mineral along the entire modeled domain.

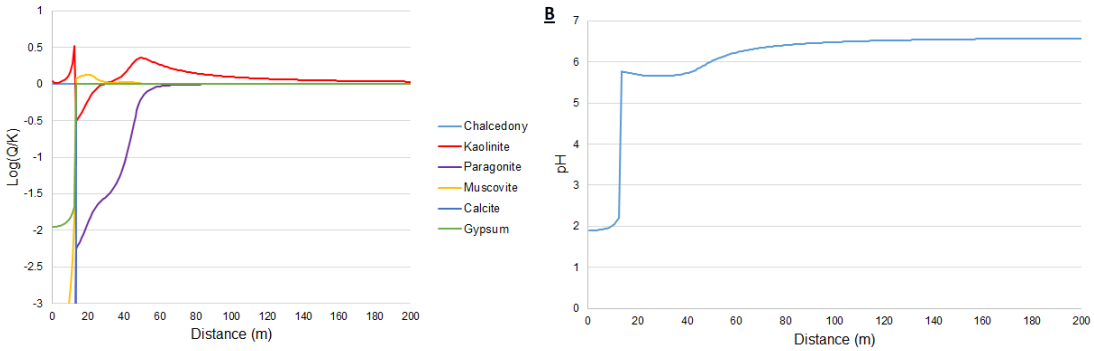


**Figure 2: (A) Mineral saturation indices and (B) corresponding pH after 1000 years of reactive transport simulation over a 200-meter long modeled domain.**

The resulting "synthetic" water was "sampled" at different points of the mesh (10, 50, 100 and 200 m) and subjected to geothermometry calculations using both GeoT and classical geothermometers. In the following section, we discuss these results in detail.

### 4.2 Multicomponent and classical geothermometry applied to synthetic waters

Results from classical and multicomponent geothermometry computations applied to synthetic water samples "collected" at 10, 50, 100 and 200 m in our modeled domain after 1000 years are illustrated in Figure 3. In the 10 m case, multicomponent geothermometry, computed with GeoT, gives a temperature of 198°C, overestimating by 48°C the simulated temperature (150°C). This discrepancy is a direct result of the lack of equilibrium between the fluid and minerals; at this distance, chalcedony is the only mineral to have reached equilibrium. Furthermore, the 6 best-clustering minerals chosen by GeoT (muscovite, Mg-beidellite, quartz, chalcedony, Ca-montmorillonite and amorphous silica; Figure 6) do not fully correspond to the minerals involved in the reactive transport simulation (paragonite, muscovite, kaolinite, chalcedony, calcite and gypsum). The Na-K geothermometer significantly overestimates the temperature (573°C) as well as the Na-K-Ca geothermometer (367°C). The K-Mg geothermometer underestimate the temperature but shows a more reasonable result (131°C). Because chalcedony remains at equilibrium within the entire modeled domain, the chalcedony geothermometer estimates perfectly the temperature (150°C) at each sampling point, while the quartz geothermometer expectedly overestimates it (173°C). With the 50 m synthetic sample, GeoT estimates the correct temperature (150°C) and identifies all simulated minerals, except kaolinite (3B). The 50 m fluid is still supersaturated with respect to kaolinite (SI = 0.35; Figure 2A). Consequently, GeoT choses a mineral which is closer to equilibrium, in this case the Mg-montmorillonite. Using the 50 m synthetic fluid composition, the Na-K, Na-K-Ca and K-Mg geothermometers significantly underestimate the modeled system temperature (111°C, 51°C and 46°C, respectively).

From 100 m on, GeoT is able to identify the correct temperature as well as all of the simulated minerals, even if the fluid is still slightly supersaturated with respect to kaolinite (Figure 2A). The Na-K, Na-K-Ca and K-Mg geothermometers grossly underestimate the system temperature (94°C, 53°C and 44°C, respectively).

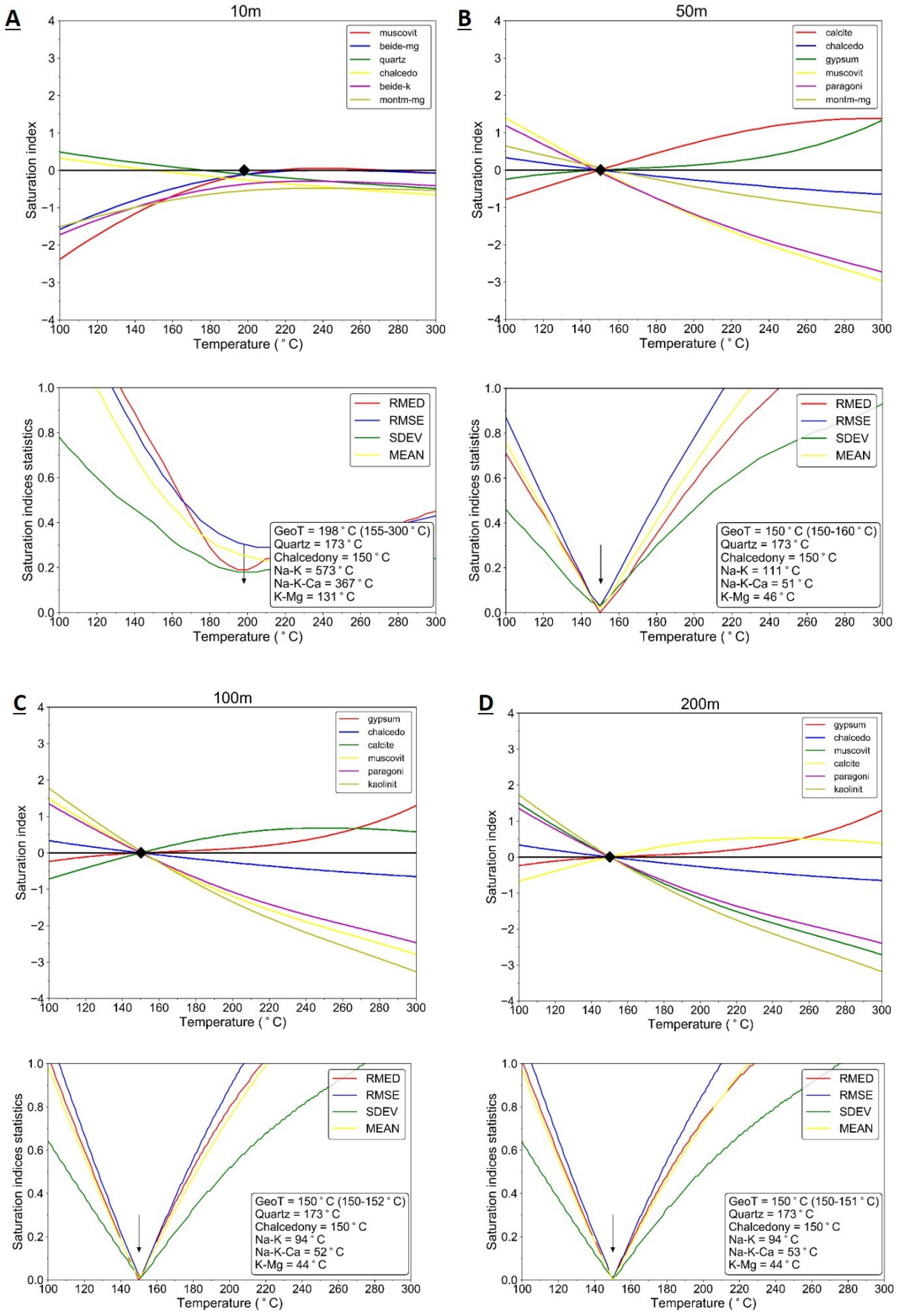


**Figure 3: Mineral saturation indices (log(Q/K)) and statistical parameters computed for the synthetic water at 10 m (A), 50 m (B), 100 m (C) and 200 m (D). RMED refers to the median, RMSE to the root mean square, SDEV to the standard deviation and MEAN to the average of the saturation indices of minerals shown, at each temperature.**

### 4.3 Sensitivity of the multicomponent method to minerals selected for geothermometry

Results from the geothermal well database analysis are expressed in percentage of correct temperature estimations (Table 5). We consider that a geothermometer provides a correct temperature estimation if the difference between the estimate and the measured reservoir temperature is within ±20°C. iGeoT provided correct estimations in 19 to 61% of all cases, depending on the minerals groups used for the computations (Table 5), while the chalcedony and Na-K geothermometers reach percentages of 34% and 4%, respectively.

**Table 5: Percentage of waters whose temperature estimation uncertainty are in a range of ±20°C.**

| Mineral group | iGeoT |
|---|---|
| 1 | 19 |
| 2 | 61 |
| 3 | 54 |
| 4 | 41 |
| 5 | 45 |
| 6 | 38 |
| 6 with Fix-Al | 53 |

Figures 4A and B shows iGeoT estimates (as well the results from chalcedony and Na-K geothermometers for comparison) for each water of the database using the mineral groups 2, 3 and numerically optimizing the Al concentration. Figure 4C illustrates the results from the Fix-Al method using the mineral group 6. Accordingly, iGeoT successfully estimates measured temperatures for more than 50% of all cases. This is a rather high number, assuming that low to medium enthalpy geothermal fluids are less likely to reach full chemical equilibrium with wall-rock minerals that high enthalpy ones. Furthermore, our analysis was not performed case-by-case, and no attempt was made to have a better constraint on the actual reservoir mineral assemblage. Although we estimated Al concentration through numerical optimization, we did not account for any secondary physical-chemical processes such as fluid mixing, boiling or chemical re-equilibration. The success of the method likely relies on the statistical approach implemented in GeoT-iGeoT. As shown theoretically with the TOUGHREACT simulation, even when the fluid is out of equilibrium with some of the minerals of the reservoir, iGeoT is capable of estimating a reasonable temperature. Another reason is that sulfates, carbonates and silica polymorphs (considered in the iGeoT runs) re-equilibrate faster (higher kinetics rate constants, Table 3) than aluminosilicates, which likely is an advantage for estimating temperature of low to medium enthalpy systems.

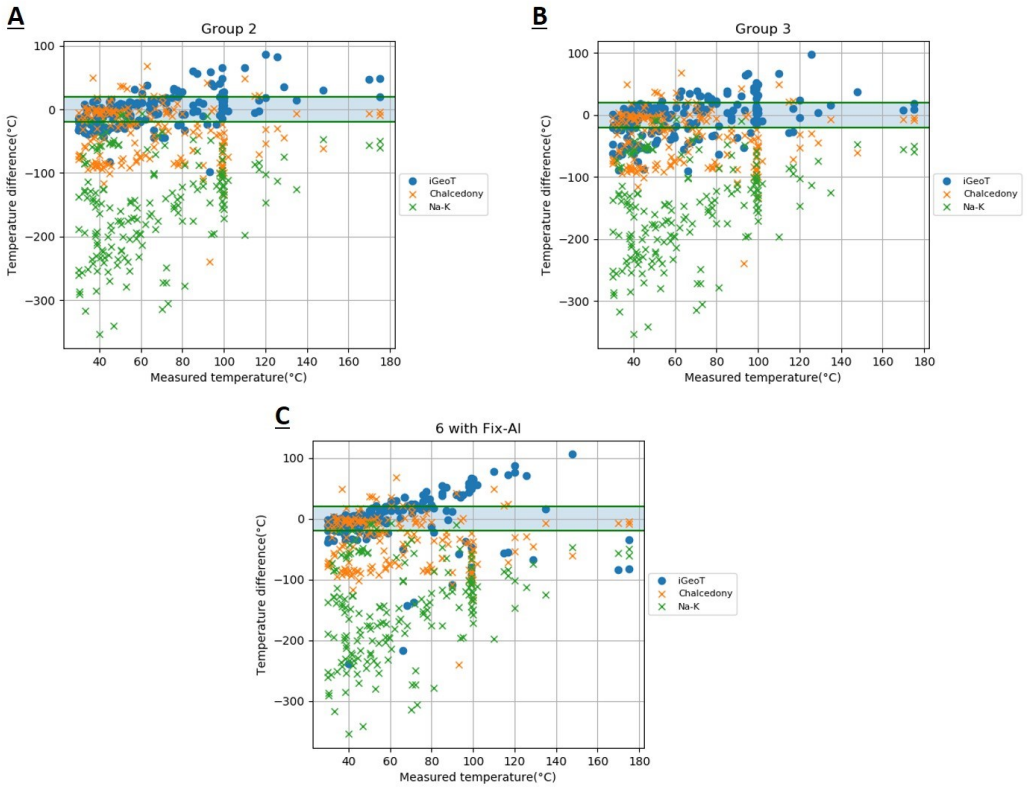


**Figure 4: Measured temperature reported in database (X-axis) vs temperature difference between measured temperature and estimated temperature by geothermometers (Y-axis). Blue stripe represents the ±20°C range of uncertainty.**

Although we obtained a high rate of reasonable temperature estimations (up to 61%), it is not expected that all the waters from the database reach equilibrium with the same groups of minerals. For this reason, iGeoT was also run with the 25 minerals from Group 6 and asked to select the 6 "best-clustering" minerals for every single water. Results from this exercise lead to a lower percentage of correct temperature estimation (38%) when using iGeoT and the grid search approach for estimating Al concentration. This is due to a limitation of the optimization process when the option to down-select "best-clustering" minerals is enabled. When a large mineral list is specified, the list down-selected minerals continuously changes during the optimization process, which can cause the objective function to become highly discontinuous and increases the likelihood of optimization convergence to a false minimum (Spycher and Finsterle, 2016). To avoid such issue, iGeoT was run with the same large group of minerals, but using the "Fix-Al" method instead of optimization to estimate the Al concentration. Al concentration was assumed to be controlled by equilibrating the fluid with microcline. In this case, a percentage of 53% of correct temperature estimations was obtained (Figure 4C). Although this percentage is significant, it must be noted that the "Fix-Al" method is sensitive to the choice of the mineral selected to fix the Al concentration.

## 5. CONCLUSION

A reactive transport model was used to simulate a case of advanced argillic alteration and create synthetic water compositions with different chemical equilibrium states, to test the response of solute geothermometers. When the fluid is far from equilibrium with minerals, the multicomponent approach computed with GeoT overestimates the reservoir temperature. However, once the fluid starts equilibrating, but still does not reach full equilibrium with all considered minerals, GeoT is able to estimate a reasonable reservoir temperature. In this theoretical study, the silica geothermometer (chalcedony) seems to the best option to estimate the temperature of the modeled reservoir, because silica has a solubility that depends mostly on temperature (not affected by acidic pH) and reaches equilibrium faster than aluminosilicates (higher kinetic reaction rate). However, for a correct application of the silica geothermometer, the user needs to have an idea of the thermal regime of the system in order to choose between the different silica geothermometer formulations (amorphous silica, chalcedony or quartz), and amount of dilution/mixing. In contrast, we showed that the multicomponent geothermometry method implemented in iGeoT is theoretically able to identify the minerals reaching equilibrium with the fluid thanks to the statistical analysis of the SI curves ("best-clustering" minerals). This is a major advantage over the silica geothermometers. The Na-K geothermometer clearly fails to estimate temperature when the dissolved concentration in Na and K is not controlled primarily by feldspars.

Regarding the solute geothermometry application to low-medium temperature systems, we showed that multicomponent geothermometry with numerical optimization can provide more accurate temperature estimations than Na-K geothermometry. The percentage of waters within ±20°C range of uncertainty was 4% for Na-K geothermometer while that of iGeoT was 19% – 61%. These results are promising considering that we did not perform a case-by-case analysis of each geothermal system contained within the database of thermal waters considered. Also, we did not perform numerical optimization of parameters besides Al concentration (e.g. concentration/dilution fractions, steam weight fractions). Performing numerical optimization of additional parameters could improve the temperature estimation. A more thorough evaluation of the mineral assemblages would also likely lead to a better performance of the optimized multicomponent approach.

## ACKNOWLEGDMENTS

This work was supported by the Conacyt project PN-2016-1998 "Exploración de sistemas geotérmicos mediante estudios geoquímicos y modelación numérica" and the Conacyt grant No. CVU: 749848. We are grateful to Michael Kühn for providing us the digital version of geothermal systems database. We are also grateful to Nathalie Collard for providing helpful comments and to Angello Hoyos for support and help with the Python code. Patrick Dobson and Nicolas Spycher were supported by the U.S. Department of Energy, Office of Energy Efficiency and Renewable Energy (EERE), Geothermal Technologies Office (GTO) under Contract No. DEAC02-05CH11231 with Lawrence Berkeley National Laboratory.

## REFERENCES

Barnes, R.B.: The Determination of Specific Forms of Aluminum in Natural Water. *Chemical Geology*, **15(3)**, (1975), 177-191.

Brunton, C., Counce, D., Bergfeld, D., Goff, F., Johnson, S., Moore, J., and Nimz, G.: Preliminary Investigation of Scale Formation and Fluid Chemistry at the Dixie Valley Geothermal Field. *Geothermal Resources Council Transactions,* **21**, (1997), 157-164.

Dobson, P.F., Kneafsey, T.J., Sonnenthal, E.L., Spycher, N., and Apps, J.A.: Experimental and Numerical Simulation of Dissolution and Precipitation: Implications for Fracture Sealing at Yucca Mountain, Nevada. *Journal of Contaminant Hydrology*, **62-63**, (2003), 459-476.

Ellis, A.J.: Chemical Geothermometry in Geothermal Systems. *Geothermics*, **25**, (1979), 219-226.

Finsterle, S.: iTOUGH2 User's Guide, Report LBNL-40040. *Lawrence Berkeley National Laboratory,* Berkeley, California, (2007).

Finsterle, S., and Zhang, Y.: Solving iTOUGH2 Simulation and Optimization Problems Using the PEST Protocol. *Environmental Modelling and Software*, **26(7)**, (2011), 959-968.

Fournier, R.O.: Chemical Geothermometers and Mixing Models for Geothermal Systems. *Geothermics*, **5**, (1977), 41-50.

Fournier, R.O.: A Revised Equation for the Na/K Geothermometer. *Geothermal Resources Council Transactions,* **3**, (1979), 221-224.

Fournier, R.O.: Application of Water Geochemistry to Geothermal Exploration and Reservoir Engineering. *In: Geothermal Systems: Principles and Case Histories. John Willey & Sons Ltd, New York,* (1981), 109-141.

Fournier, R.O.: The Behavior of Silica in Hydrothermal Solutions. *Review in Economic Geology,* **2**, (1985), 45-61.

Fournier, R.O.: Lectures on Geochemical Interpretation of Hydrothermal Waters. *UNU Geothermal Training Programme,* Report **10**, (1989), 73 p.

Fournier, R.O. and Truesdell, A.H.: An Empirical Na-K-Ca Geothermometer for Natural Waters. *Geochimica et Cosmochimica Acta,* **37**, (1973), 1255-1275.

Fournier, R.O., White, D.E. and Truesdell, A.H.: Geochemical Indicators of Subsurface Temperature- Part 1, basic assumptions. *Journal Research US Geological Survey*, **2**, (1974), 259-262.

Fournier, R.O., and Potter, R.W.: A Revised and Expanded Silica (Quartz) Geothermometer. *Geothermal Resources Council Bulletin,* **Nov.**, (1982), 3-12.

Giggenbach, W.F.: Geothermal Solute Equilibria: Derivation of Na-K-Mg-Ca Geoindicators. *Geochimica et Cosmochimica Acta,* **52**, (1988), 2749-2755.

Giggenbach, W.F., Gonfiantini, R., Jangi, B.L., and Truesdell, A.H.: Isotopic and Chemical Composition of Parbati Valley Geothermal Discharges, N. W. Himalaya, India. *Geothermics*, **12**, (1983), 199-222.

Goff, F., Bergfeld, D., Janik, C.J., Counce, D., and Murrell, M.: Geochemical Data on Waters, Scales and Rocks from the Dixie Valley Region, Nevada. *Los Alamos National Laboratory Report,* (2002).

Kaasalainen, H., and Stefánsson, A.: The Chemistry of Trace Elements in Surface Geothermal Waters and Steam, Iceland. *Chemical Geology,* **330**, (2012), 60-85.

Kristmannsdóttir, H.: Types of Scaling Occurring by Geothermal Utilization in Iceland. *Geothermics,* **18 (1-2)**, (1989), 183-190.

Kuhn, M.: Reactive Flow Modeling of Hydrothermal Systems: Concepts, Classification and Chemistry of Geothermal Systems. *Springer,* (2004), 10-165.

Lasaga, A.C., Soler, J.M., Ganor, J., Burch, T.E., and Nagy, K.L.: Chemical Weathering Rate Laws and Global Geochemical Cycles. *Geochimica et Cosmochimica Acta,* **58**, (1994), 2361-2386.

Nicholson, K.: Geothermal Fluids: Chemistry and Exploration Techniques. *Springer New York,* (1993), 263 p.

Palandri, J.L., and Kharaka, Y.K.: A Compilation of Rate Parameters of Water-Mineral Interaction Kinetics for Application to Geochemical Modeling. *U.S. Geological Survey Open File Report,* **2004-1048**, (2004), 64 p.

Palmer, C.D., Ohly, S.R., Smith, R.W., Neupane, G., McLing, T., and Mattson, E.: Mineral Selection for Multicomponent Equilibrium Geothermometry. *Geothermal Resources Council Transactions,* **38**, (2014), 453-459.

Pang, Z.H., and Reed, M.H.: Theoretical Chemical Thermometry on Geothermal Waters: Problems and Methods. *Geochimica et Cosmochimica Acta,* **62**, (1998), 1083-1091.

Peiffer, L., Wanner, C., Spycher, N., Sonnenthal, E.L., Kennedy, B.M. and Iovenitti, J.: Optimized Multicomponent vs. Classical Geothermometry: Insights from Modeling Studies at the Dixie Valley Geothermal Area. *Geothermics,* **51**, (2014), 154-169.

Pruess, K.: TOUGH2- A General-Purpose Numerical Simulator for Multiphase Fluid and Heat Flow. Rep. LBL-29400. Lawrence Berkeley National Laboratory, Berkeley, CA (1991).

Reed, M.H.: Hydrothermal Alteration and its Relationship to Ore Fluid Composition. *Geochemistry of hydrothermal ore deposits*, **3**, (1997), 303-365.

Reed, M.H., and Spycher, N.: Calculation of pH and Mineral Equilibria in Hydrothermal Waters with Application to Geothermometry and Studies of Boiling and Dilution. *Geochimica et Cosmochimica Acta,* **48 (7)**, (1984), 1479-1492.

Reed, M.H., and Palandri, J.L.: SOLTHERM.H06, A Database of Equilibrium Constants for Minerals and Aqueous Species. Available from the authors, University of Oregon, Eugene, USA, (2006).

Regenspurg, S., Feldbusch, E., Byrne, J., Deon, F., Driba, D.L., Henninges, J., Kappler, A., Naumann, R., Reinsch, T., and Schubert, C.: Mineral Precipitation during Production of Geothermal Fluid from a Permian Rotliegend Reservoir, *Geothermics,* **54**, (2015), 122-135.

Rimstidt, J.D.: Quartz Solubility at Low Temperatures. *Geochimica et Cosmochimica Acta*, **61(13)**, (1997), 2553-2558.

Rimstidt, J.D., and Barnes, H.: The Kinetics of Silica-Water Reactions. *Geochimica et Cosmochimica Acta*, **44(11)**, (1980), 1683-1699.

Spycher, N., Peiffer, L., Sonnenthal, E.L., Saldi, G., Reed, M.H., and Kennedy, B.M.: Integrated Multicomponent Solute Geothermometry, *Geothermics,* **51**, (2014), 113-123.

Spycher, N., and Finsterle, S.: iGeoT v1.0: Automatic Parameter Estimation for Multicomponent Geothermometry, User's Guide. *Lawrence Berkeley National Laboratory,* Berkeley, California, (2016).

Steefel, C.I., and Lasaga, A.C.: A Coupled Model for Transport of Multiple Chemical Species and Kinetic Precipitation/Dissolution Reactions with Applications to Reactive Flow in Single Phase Hydrothermal System. *American Journal of Science*, **294**, (1994), 529-592.

Truesdell, A.H.: Summary of Section III. Geochemical Techniques in E<xploration. *Proceedings 2nd UN Symposium on the development and use of geothermal resources, San Francisco, 1975,* **1**, (1976), 103-129.

Wanner, C., Eichinger, F., Jahrfeld, T., and Diamond, L.W.: Causes of Abundant Calcite Scaling in Geothermal Wells in the Bavarian Molasse Basin, Southern Germany. *Geothermics*, **70**, (2017), 324-338.

White, D.E.: Geochemistry Applied to the Discovery, Evaluation and Exploitation of Geothermal Energy Resources. *Geothermics*, *Special Issue 2,* **1**, (1970), 58-80.

Xu, T., Sonnenthal, E.L., Spycher, N., and Zheng, L.: TOUGHREACT V3.0-OMP Reference Manual: A Parallel Simulation Program for Non-Isothermal Multiphase Geochemical Reactive Transport. LBNL Manual: http://esdl.lbl.gov/FILES/research/projects/tough/documentation/TOUGHREACT_V3-OMP_Ref.Manual.pdf. (2014). Accessed January 2019.

Zarrouk, S.J., Woodhurst, B.C., and Morris, C.: Silica Scaling in Geothermal Heat Exchangers and its Impact on Pressure Drop and Performance: Wairakei binary plant, New Zealand, *Geothermics,* **51**, (2014), 445-459.